# Three-dimensional boundary layer transition study

**Y. P. Kohama**

Institute of Fluid Science, Tohoku University, 2-1-1 Katahira, Sendai 980-8577, Japan

**The present investigation deals with the boundary layer transition problem in relation to the fundamental aerodynamics of general airplanes. Focus has been especially placed on the mechanism of three-dimensional (3D) boundary layer transition and its control, which is meaningful not only for its fundamental interest but also important in relation to aero- and hydro-dynamic applications. In order to clarify the complicated transition mechanism, both flow visualizations and hot wire measurements are conducted in the transition region of general 3D boundary layer flows, namely, on spinning, yawed, and curved surfaces of the kind that often appear in surfaces of industrial fluid machinery. A unique attempt to delay such transition, applying an effective control method, is also reported.**

## Introduction

It is more than 30 years since the last epoch-making commercial airplane B-747 was developed and constructed in 1969. This implies that the B-747 was such an excellent plane that it has been difficult to design a more elaborate one easily. However, taking into account the present serious environmental problem introduced by the greenhouse effect, further development of conventional planes should attempt to reduce $CO_2$ emission. It is rather easy for cars, trains and ships to switch their fuel from petroleum to other alternative ones. However, it is a much more difficult thing for airplanes to do it. Therefore the only thing we can do in the case of the airplane is to reduce its drag as much as possible.

Laminar Flow Control (LFC) technology is still under way although it was started over 50 years ago. The main reason is that the transition mechanism is quite different in the case of 3D boundary layers, and very complicated. Control devices, like the uniform suction of the boundary layer as in the case of the two-dimensional (2D) boundary layer[1], are not always effective in the case of 3D boundary layers like a swept wing flow. Passive control[2], which was again effective in the case of the 2D boundary layer, is not always effective in the case of a 3D boundary layer. According to one estimate, up to 25% of fuel consumption will be saved if the full lifting surface of the main wing of a large aircraft like B-747 is kept laminar by possible LFC technology. This means that up to 40 tons of fuel (equivalent weight to the pay load) can be unloaded at the take off condition. From such economical and environmental backgrounds, 3D boundary layer transition study is considered to be important especially in those countries that have an aircraft industry. A review of the 3D boundary layer studies is available in ref. 3.

e-mail: kohama@ltwt.ifs.tohoku.ac.jp

## Brief history of 3D transition studies

The history of 3D boundary layer transition studies is rather old. Taylor[4] investigated the flow in a gap between two cylinders. He observed a counter rotating vortex system in the gap flow. Centrifugal force drives the laminar flow unstable and a streamwise vortex structure starts to appear as the primary instability. Goertler[5] calculated the stability characteristics of the boundary layer on a concave wall, which is the simplified shape of the pressure surface of some wings, and predicted early transition by a streamwise vortex system called later the 'Goertler vortex'. Such transitions are in general called the 'Taylor–Goertler instability'. Bippes[6] visualized the Goertler instability clearly and showed the appearance of a secondary instability in the later stages of the transition. Aihara and Koyoma[7] and Ito[8] followed with experimental investigations and showed the relation between the Goertler vortex and the appearance of the secondary instability. Swearingen and Blackwelder[9] showed that there appear two different modes in the secondary instability, the sinuous mode and the varicose mode. Bahri *et al.*[10] studied the nature of the secondary instability with respect to pressure along the flow. In accelerated flow the sinuous mode appears, while in decelerated flow the varicose mode appears. They also concluded that the most dangerous mode which brings transition to turbulence is the varicose mode. Boundary layer transition characteristics on a concave/convex curved wall with yaw was investigated by Kohama[11]. This was a simplified model of the lower part of the leading edge of a unique laminar flow wing configuration designed by NASA Langley[12]. Owing to the yaw angle, boundary layer transition changed from Goertler type to crossflow type. A two-stage transition process (primary and secondary instability) was detected both by hot wire and flow visualization.

Gregory *et al.*[13] worked on a spinning disk flow and visualized a spiral vortex structure in the transition

process by the china-clay method. This study was a series of investigations after Gray's[14] flight test. (Swept wing flow and spinning disk boundary layer flow are initially similar.) Following this, more general boundary layer transition studies on spinning bodies have been done by many researchers. Kohama[15–17], and Kobayashi and Izumi[18] visualized the spatial transition structure using the smoke technique. Figure 1 *a–d* shows boundary layer transition on spinning bodies. A co-rotating vortex structure is visible from the close-up photo in the case of the spinning disk, while it looks like a counter-rotating structure in the case of a spinning cone ($2\theta = 30^\circ$, $2\theta = 60^\circ$) in uniform flow. Owing to the included half angle $\theta$, the driving force of the transition changes from pure crossflow type at around $\theta = 0^\circ$ (cylinder) to pure centrifugal type at $\theta = 90^\circ$ (disk). Between these limits, two instabilities exist at the same time in the flow region. At around $\theta = 60^\circ$, the magnitude of the driving force changes. In the case of an ogive nose cone, Mueller[19] visualized the transition region by smoke, and detected simultaneous appearance of both crossflow and T–S wave instabilities after the corner between cone and cylinder. In the case of ogive-cones, as shown in Figure 2 *a–d* with and without uniform flow, the transition process seems to be quite different. Transition seems to be delayed in the case of concave cones with respect to convex cones. In the case of concave cones, centrifugal force acting towards the body surface seems to stabilize the transition.

Gray[14] was the first to observe streamwise crossflow vortices on a swept wing surface while flight tests were being conducted in 1952. Since then, a new instability called crossflow instability has been recognized, and systematic investigations started. Poll[20,21] investigated the crossflow instability using a yawed cylinder and visualized the crossflow vortex system by the oil flow method. He also measured two different unsteady modes by hot wire, in the later stages of the transition region. From his investigation, unsteady crossflow modes were first recognized, namely, an unsteady low frequency mode at 1 kHz and a high frequency mode at 17.5 kHz. The interesting point at this stage is the relation between stationary streamwise vortices and the unsteady instabilities. Kohama and Motegi[22] investigated a similar flow field experimentally using hot wires and several different flow visualization techniques including temperature-sensitive liquid crystals. He also observed unsteady modes and clarified the effect of the yaw angle. Figure 3 shows the liquid crystal visualization results. Crossflow instability seems to be most amplified at around $\Lambda = 57^\circ$.

Experimental investigation of the crossflow-dominant transition on a real swept wing model is very difficult. Transition occurs near the leading edge where the boundary layer is very thin and velocity is fairly high. Furthermore, the wall has strong curvature and yaw

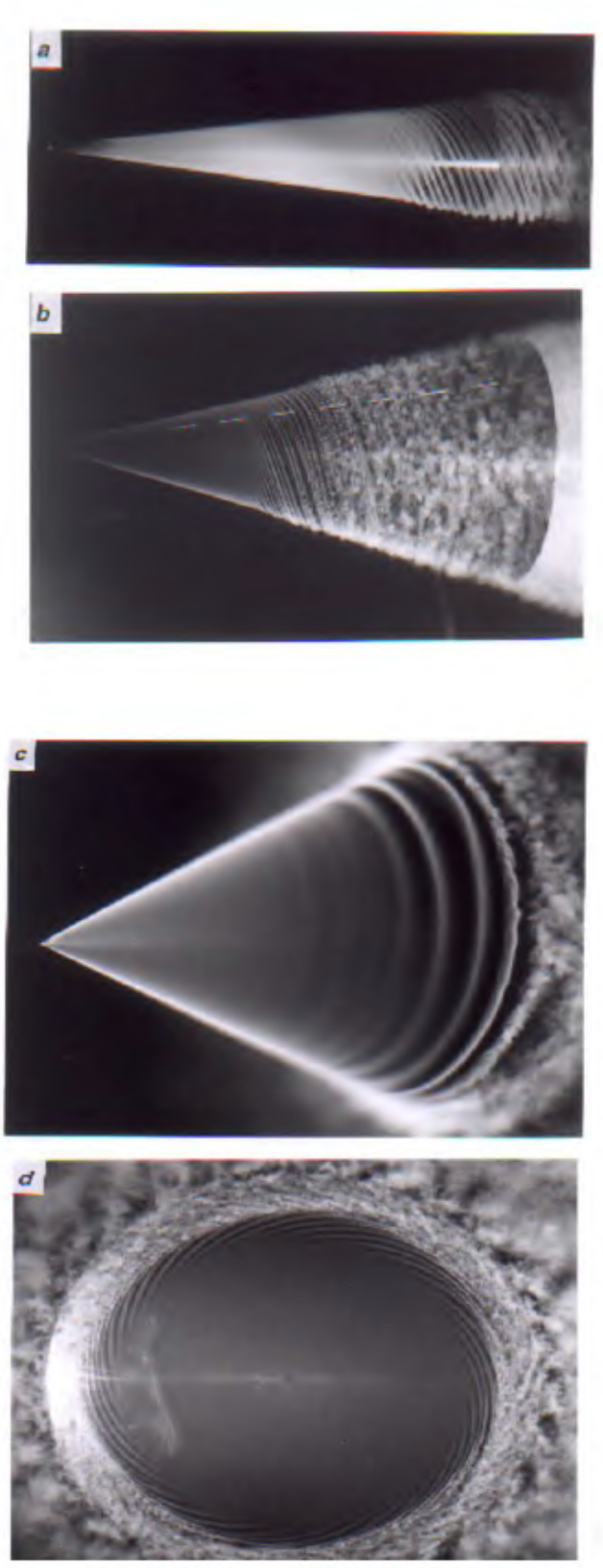


**Figure 1.** Flow visualization of spinning cones (Titanium tetra chloride smoke visualization). ***a***, $2\theta = 15^\circ$ ($U_\infty = 1.8$ m/s, $N = 1{,}000$ rpm, $L = 300$ mm); ***b***, $2\theta = 30^\circ$ ($U_\infty = 1.7$ m/s, $N = 670$ rpm, $L = 370$ mm); ***c***, $2\theta = 60^\circ$ ($U_\infty = 0$ m/s, $N = 700$ rpm, $L = 250$ mm); ***d***, $2\theta = 180^\circ$ ($U_\infty = 0$ m/s, $N = 1{,}800$ rpm, $L = 400$ mm).

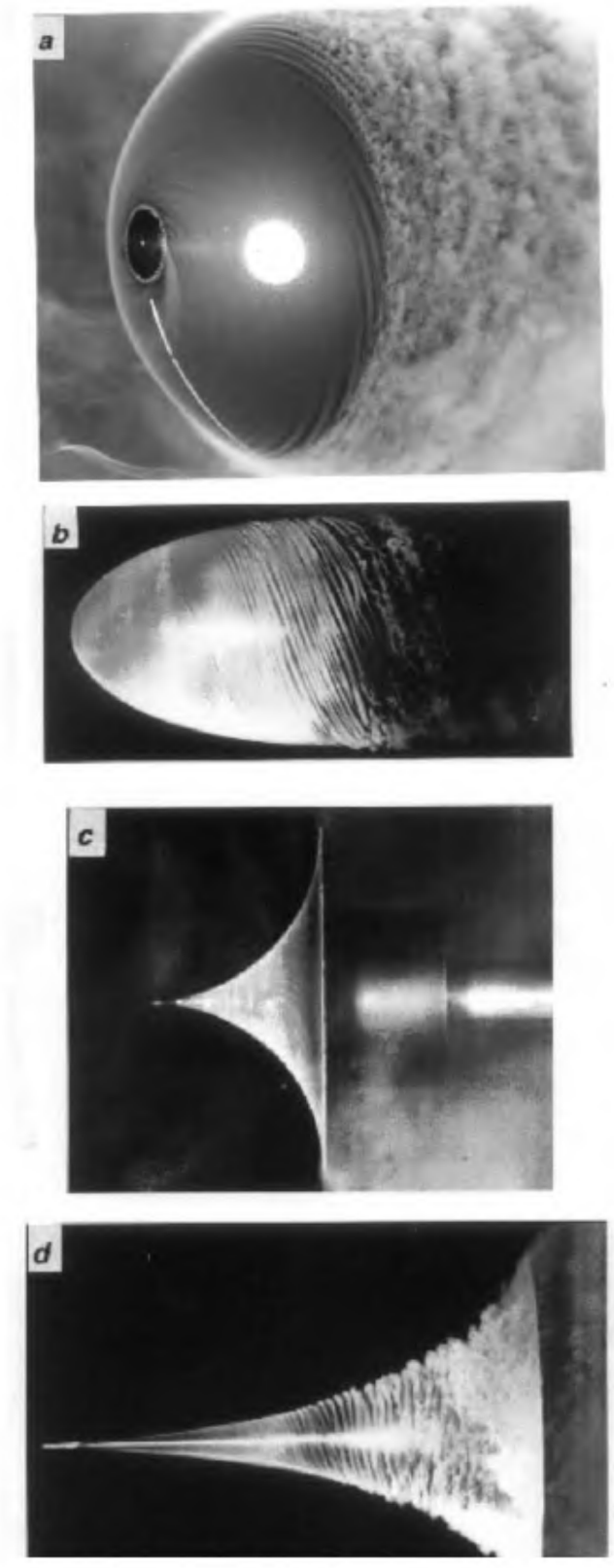


**Figure 2.** Flow visualization of spinning ogive–cones (Titanium tetra chloride smoke visualization). ***a***, Sphere ($N$ = 3,200 rpm, $D$ = 250 mm); ***b***, Concave–Ogive–Cone ($N$ = 500 rpm, $D$ = 150 mm, ratio 1:2); ***c***, Convex–Ogive–Cone ($N$ = 2,000 rpm, $D$ = 150 mm, ratio 1:1); ***b***, Convex–Ogive–Cone ($N$ = 2,000 rpm, $D$ = 150 mm, ratio 1:2).

angle. In order to solve such difficulties, Saric and Yeats[23] introduced a clever experimental model which gives a transition region similar to that on a swept wing, namely, a yawed flat plate with an upper displacement body model. With this model, most of the difficulties involved in a swept wing are solved on a flat surface with a thick boundary layer. Saric and Yeats visualized the flow field by the naphthalene method and conducted fine velocity measurements by the hot wire method. Nonlinear development of the crossflow vortices showed 'wave doubling' in the velocity field, namely, the wavelength of the vortices changed to half of the original values as they develop downstream.

Kohama *et al.*[24,25] were the first to tackle real swept wing flow. They introduced a natural laminar flow wing with negative angle of attack so that the transition region can be broadened and boundary layer can be thickened. Finally, the angle of attack was selected at $\alpha = -5^{\circ}$. Using this model they measured complicated three-dimensional transition structures and clarified the process in detail. They also pointed out the origin where the two different unsteady modes will start to appear. According to their results, the low frequency mode starts to appear at the point where the point of inflection exists in the $U(z)$ velocity profile, and the high frequency mode at the point where the point of inflection exists in the $U(y)$ velocity profile. Using these experimental results, they also sketched the relation between the stationary vortex structure (primary instability) and the unsteady modes. Figure 4 shows a sketch of the complicated transition region.

Boundary layers developing on compressor or turbine blades experience high turbulence intensity in the oncoming flow. Under such conditions, the transition process will change from conventional T–S wave 2D transition. In relation to such a problem, Alfredsson and Matsubara[26] investigated flat plate boundary layer transition under high turbulence levels. They visualized the transition field by smoke and showed clear streamwise vortex structures. The process seems to be quite similar to that of Goertler transition. A secondary instability stage is also observed. This transition process is called bypass transition.

In relation to atmospheric phenomena, boundary layer transition on a heated wall was also investigated by many scientists. Kohama and Ohta[27] visualized the flow and observed streamwise vortex structures in the boundary layer. The visualized flow pattern is shown in Figure 5 *a*, *b*. Similar structures can often be observed in atmospheric flow, as shown in the photograph taken from satellites in the same figure. In Japan, heavy snow fall occurs in the west coast of the country along the Japan Sea. It is considered that the vortex structure in the Japan Sea enhances entrainment of the water from the sea into the air while there is north-westerly flow from Siberia to Japan. The temperature difference

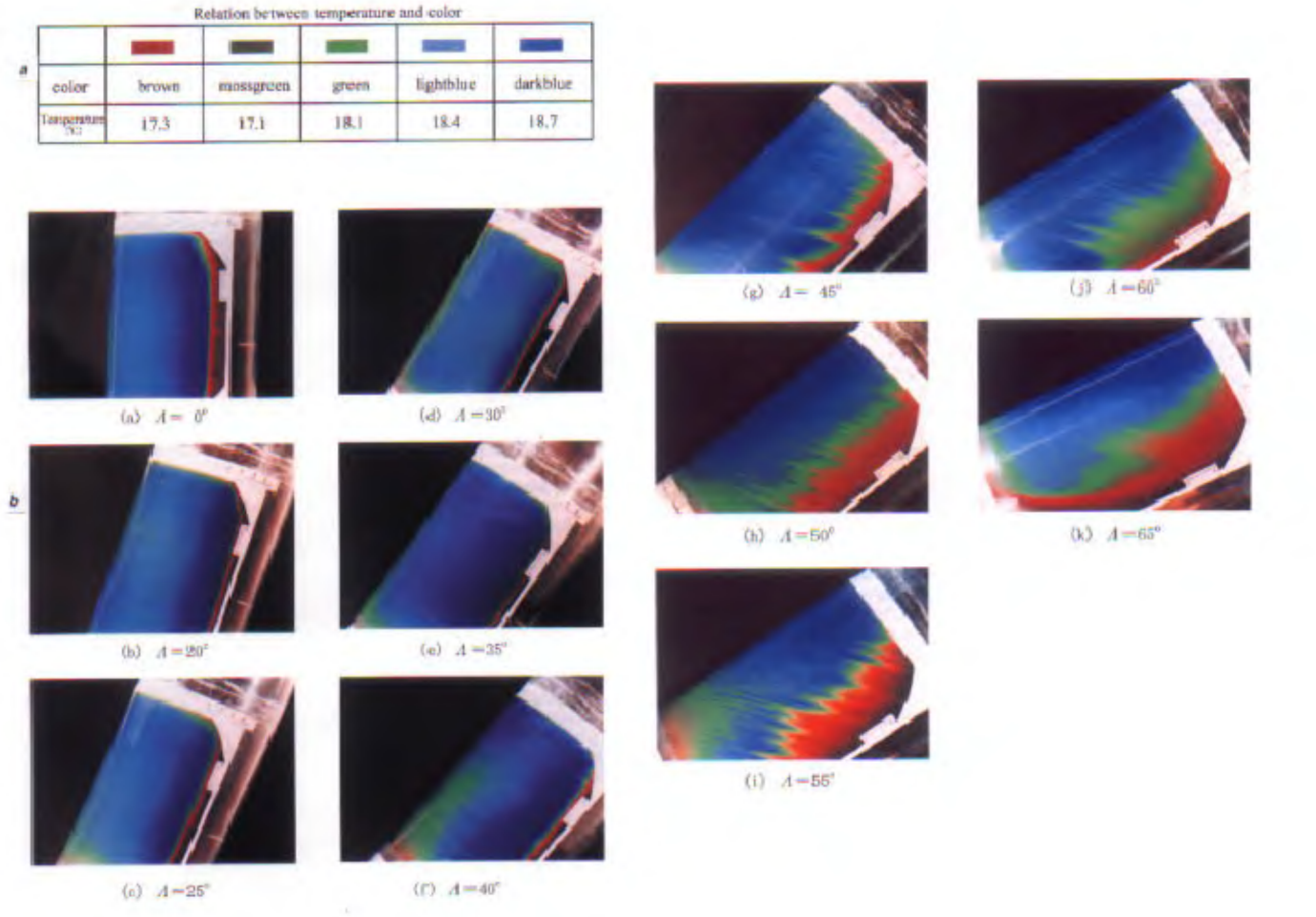


**Figure 3.** Flow visualization of a yawed cylinder (temperature-sensitive liquid crystal visualization, $U_\infty = 40$ m/s, $D = 300$ mm). ***a***, Relation between temperature and colour; ***b***, Appearance of crossflow vortices with respect to yaw angle Λ.

between air and water in the Japan Sea is very large; sometimes it goes up over $\Delta T = 65^\circ$. It drives the generation of Goertler vortex-like streamwise vortices in the atmospheric boundary layer and enhances the snow fall.

## Three dimensional boundary layer transition mechanism

We have investigated 3D boundary layer transition on several different experimental models. 3D boundary layer flows can be summarized into three categories.

(1) Boundary layer on spinning body surface.
(2) Boundary layer on curved body surface.
(3) Boundary layer on yawed body surface.

The transition process seems to be different in each of the different models. However, studying the results of many other investigations and comparing with our own results, we came to the conclusion that there exists a consistent transition process: the streamwise vortex appears as the primary instability and the unsteady mode appears as a secondary instability[28]. After the appearance of the secondary instability, the boundary layers shift to fully turbulent boundary layers.

### *Primary instability stage*

The streamwise vortex structure appears as the primary instability. The vortices may be either co-rotating or counter-rotating, depending on the direction of the external force relative to the wall surface. The vortex motion of the stationary streamwise vortex structure deforms the uniform 2D laminar boundary layer flow into a complicated 3D structure[24]. In the case of a counter-rotating the structure deformation is quite symmetric, while it is quite anti-symmetric in the case

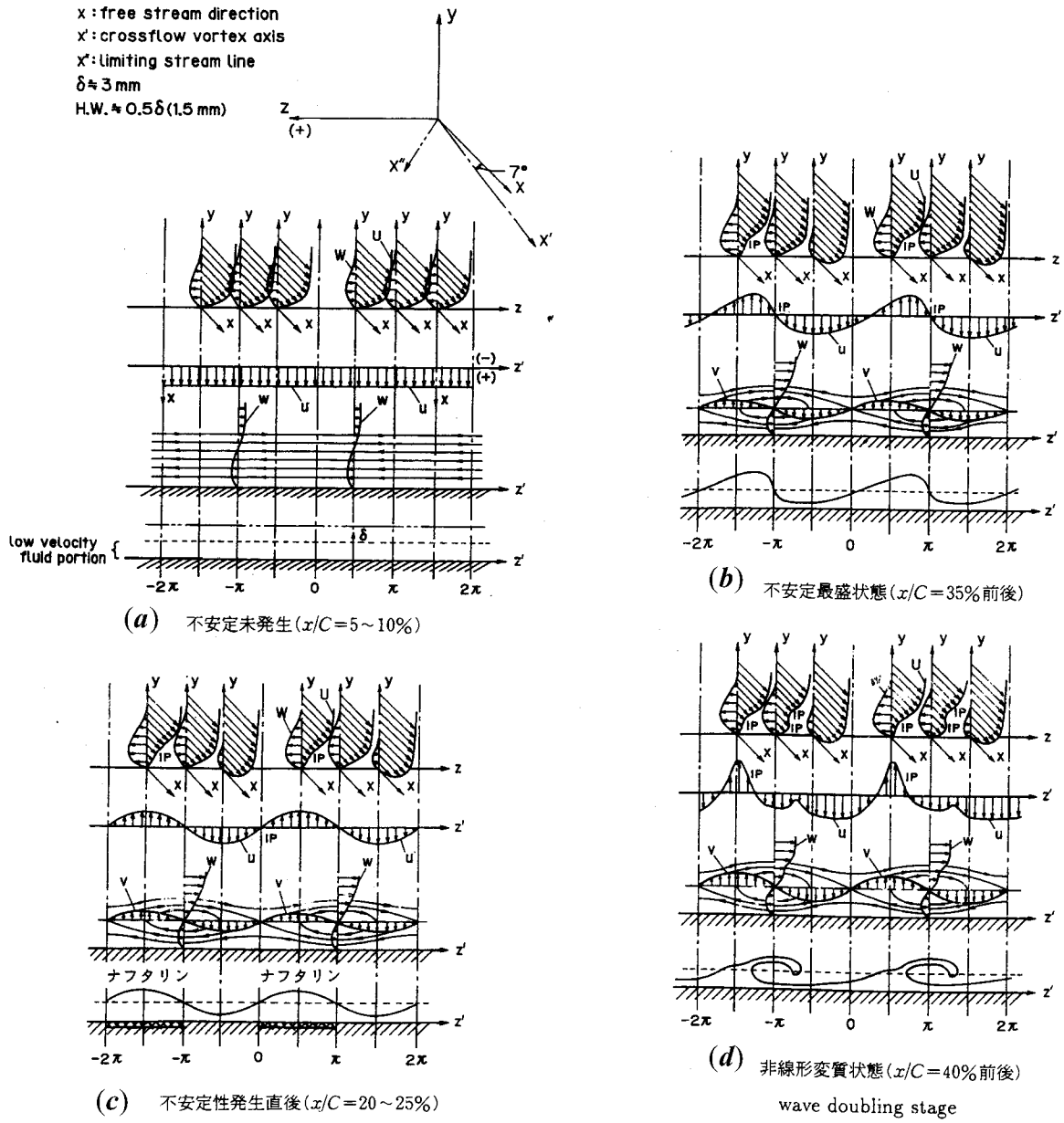


**Figure 4.** Complicated crossflow transition process. ***a***, Sub-critical condition ($x/C$ = 5~10%); ***b***, After the critical condition ($x/C$ = 20~25%); ***c***, Transition, linear stage ($x/C$ = 35%); ***d***, Nonlinear stage ($x/C$ = 45%).

of co-rotating structures (crossflow instability). As a result, highly unstable conditions for inflectional instability start to appear both in $U(z)$ and $V(y)$ velocity profiles.

## *Secondary instability stage*

In the case of the counter-rotating structure, a sinuous mode will appear when the point of inflection in the $U(z)$ profile is more unstable than the $V(y)$ profile. The varicose mode appears when the point of inflection in the $U(y)$ profile is more unstable than the $U(z)$ profile to the secondary instability. In the case of the co-rotating structure, the low frequency unsteady primary mode will appear when the point of inflection in the $U(z)$ profile becomes unstable, while a high frequency unsteady secondary mode will appear when the point of inflection in the $U(y)$ profile becomes unstable. The reason why the appearance of the secondary instability is different in the two cases is the existence of the crossflow velocity component in the case of the co-rotating structure[29]. A visualization of the cross-sectional flow structure is shown in Figure 6. Another reason is that the height of

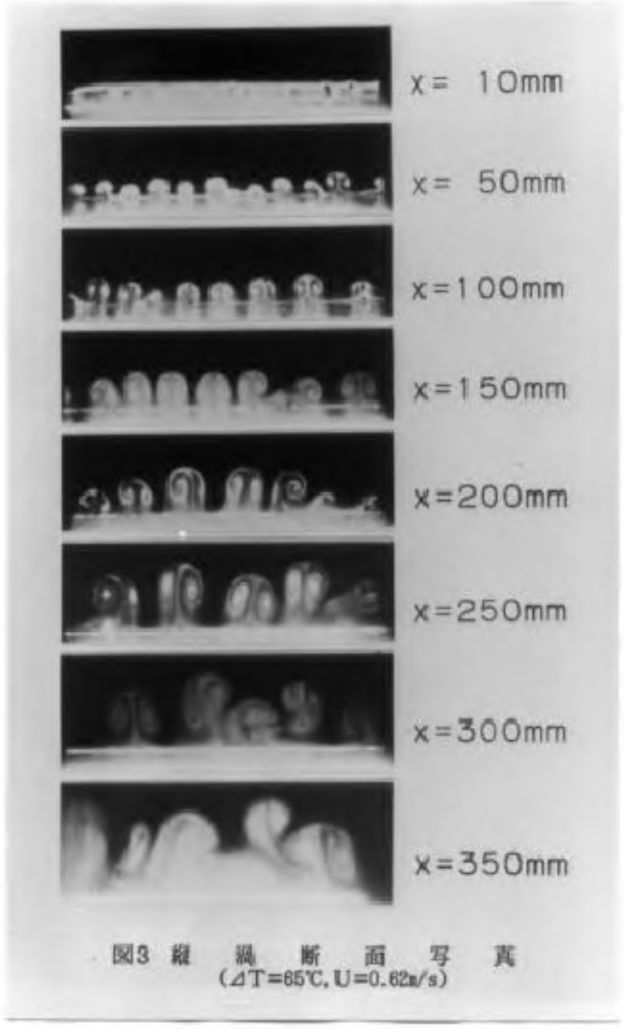


**Figure 5 *a***, Streamwise vortex system appearing on a heated water surface. Experiment ($\Delta T = 65°$, $U_\infty = 0.62$ m/s).

the points of inflection in the $U(y)$ and $U(z)$ profiles are different in the case of the co-rotating structure[30]. The point of inflection in $U(z)$ is very low and the velocity there is also fairly slow. In the counter-rotating case, on the other hand, the heights are about the same. Of course the point in $U(y)$ is higher than that in $U(z)$ and therefore the frequency is higher in the case of the varicose mode, but the difference is not large compared to that of the co-rotating case.

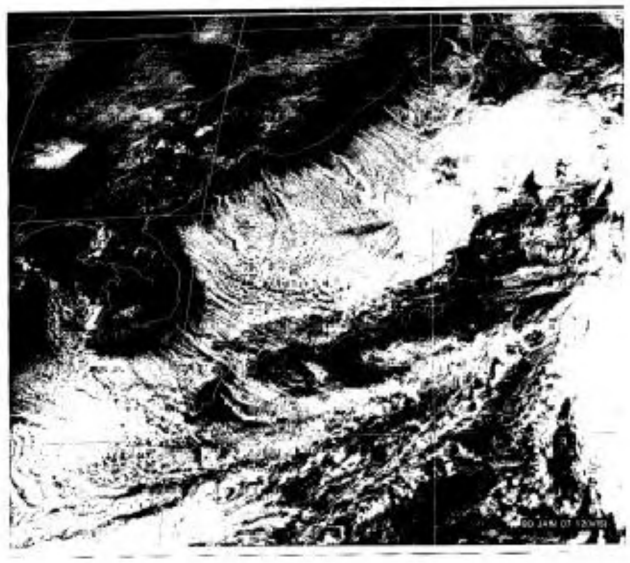

**Figure 5 *b***, Streamwise vortex system appearing on a heated water surface. Flow over Japan Sea (Winter, taken from a satellite).

## Possible laminar flow control methods

Passive laminar flow control of the 3D boundary layer can be achieved also by designing the pressure distribution on the suction side of the wing to accelerate the flow gradually as much as one can. Reduction of the sweep angle is also effective, but it compromises the cruise speed, slowing it down at a certain level of sweep.

Uniform suction of the boundary layer at the leading edge area is considered to be effective also for the 3D case. However, the suction structures create a receptivity mechanism[31]. So application of active control devices to the leading edge area is very dangerous. Saric *et al.*[32] showed a unique method of control of the boundary layer when they placed a micron-sized roughness array at the position where the boundary layer becomes unstable with a pitch that is smaller than the natural wavelength. By doing so, steady crossflow vortices appear with very small height. As a result, appearance of the secondary instability downstream is delayed, and eventually transition to turbulence is also delayed. Kohama and Egami[33] on the other hand applied an effective selective suction system. Taking into account the streamwise stationary crossflow structure, suction slits are grooved at the foot of each streamwise vortex. The low momentum flow which would otherwise have existed at the bottom of the laminar boundary layer is gathered to the vortex motion of the foot of each streamwise vortex. Through delicate measurements, it

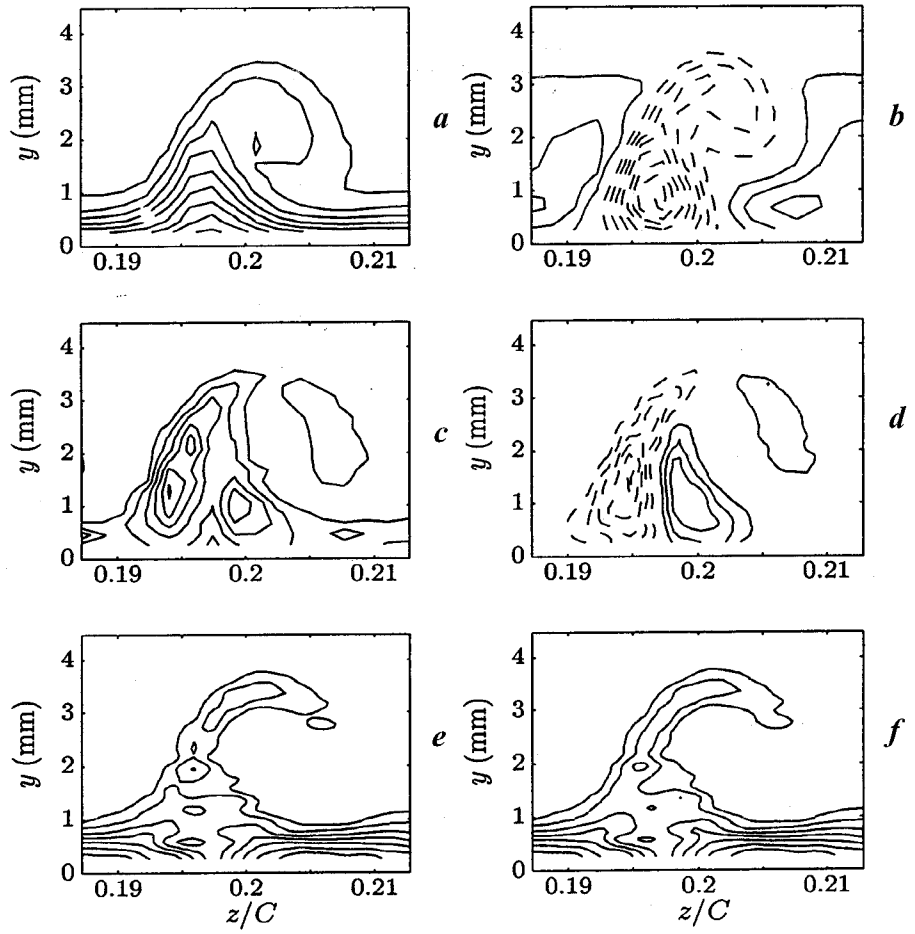


**Figure 6.** Cross-sectional velocity field of a crossflow transition region. Contours of (*a*) $\overline{U}/U_e$, (*b*) $\overline{U}_s/U_e$, (*c*) $u_{rms}/U_e$, (*d*) $d(\overline{U}/U_e)/d(z/C)$, (*e*) $d(\overline{U}/U_e)/d(y/C)$, (*f*) $[(d(\overline{U}/Ue)/d(y/C))^2+(d(\overline{U}/Ue)/d(z/C))^2]^{1/2}$, in $yz$-plane at $x/C = 0.5$. Contour interval is 0.1 $U_e$ for (*b*), ± 0.05 $U_e$ for (*b*), 0.02 $U_e$ for (*c*), ± 30 for (*d*), and 90 for (*d*). Dashed lines correspond to negative values. The roughness array with 12.5 mm pitch is placed at $x/C = 0.17$.

has already been shown that this low momentum flow creates the unstable flow condition for the onset of the secondary instability in the $U(y)$ profile. Therefore, if the low momentum flow is gathered and selectively sucked by those suction slits with less power than uniform suction, the transition will be delayed[33]. Following such considerations, selective suction was applied on a yawed flat wall with an upper displacement body model, and transition was successfully delayed with 1/3 of suction power compared to uniform suction. Figure 7 *a–c* show the results obtained. Figure 7 *a* shows the condition without suction while Figure 7 *b*, *c* show the condition with suction. The effect is quite clear from the figures. Figure 7 *c*, the line suction case, is the most effective.

## Concluding remarks

Some kind of laminar flow control technique must be applied to the main wing of the next generation large subsonic aircraft in order to reduce fuel consumption. It is even more essential for next generation supersonic transports to improve their lift to drag ratio. An elaborate laminar flow control technique is therefore a strong possibility.

It is only recently that the complicated transition mechanism in 3D boundary layers has started to reveal its true structure. Still many discussions are going on and several possible scenarios have been proposed by many scientists. However, we believe that the major transition process which is important for the control

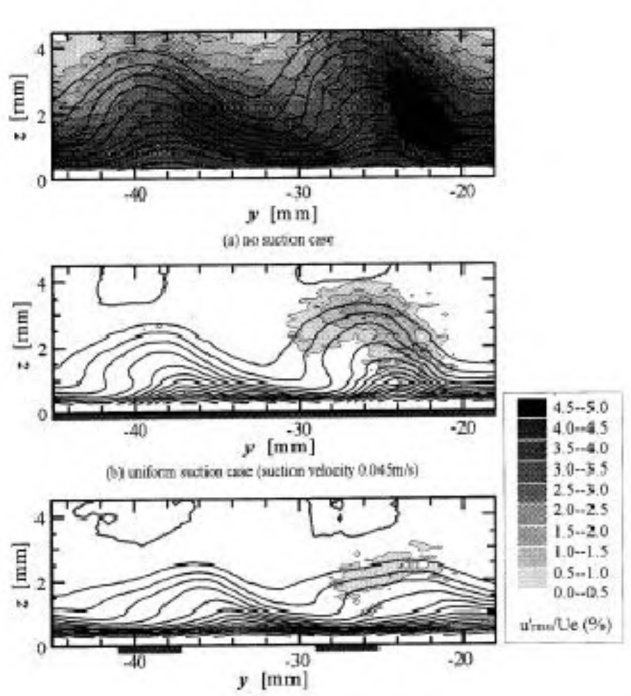


**Figure 7.** Effect of selective suction on a crossflow transition field (velocity contour line step is 5% of $U_e$, Bandpass filter range: 1.25–3 kHz for disturbance $f_2$, $x/C = 0.79$, $U_\infty = 12.3$ m/s, Suction volume 0.045 $m^3/m^2 \cdot s$. ***a***, no suction case; ***b***, uniform suction case (suction velocity 0.045 m/s); ***c***, selective suction case (suction velocity 0.124 m/s).

technique is the appearance of the stationary streamwise vortex structure. This process is generally accepted by many scientists and can be considered as the general process. Therefore, one must more or less take into account this structure when controlling the boundary layer to delay transition or to enhance some mass transfer rates.


1. Schubauer, G. B. and Skramstad, H. K., NBS Research Paper 1772, 1943.
2. Althaus, D., Stuttgarter Profilkatalog, Inst. Aerodynamik Stuttgart Univ., 1972.
3. Reed, H. L. and Saric, W. S., *Annu. Rev. Fluid Mech.*, 1989, **21**, 235–284.
4. Taylor, G. I., *Philos. Trans.*, 1923, **223**, 289–343.
5. Goertler, H., *Nachr. Wiss. Ges. Goettingen, Math. Phys. Klasse, Neue Folge*, 1940, **2**.
6. Bippes, H., *Acta Mech.*, 1972, **14**, 251–267.
7. Aihara, Y. and Koyama, H., *Trans. Jpn. Soc. Aero. Space Sci.*, 1981, **24**, 78–94 (in Japanese).
8. Ito, A., *Trans. Jpn. Soc. Aero. Space Sci.*, 1985, **33**, 58–65 (in Japanese).
9. Swearingen, J. D. and Blackwelder, R., *J. Fluid Mech.*, 1987, **182**, 255–292.
10. Bahri, F. *et al.*, Proceedings of the IUTAM Symposium on Laminar–Turbulent Transition, Kluwer, Dordrecht, 2000, to be published.
11. Kohama, Y., *Turbulence Management and Relaminarization* (eds Liepmann, H. W. and Narasimha, R.), Springer-Verlag, 1988, pp. 215–226.
12. Pfenninger, W., Reed, H. L. and Dagenhart, J. R., *Prog. Astro. Aero.*, 1980, **72**, 249–271.
13. Gregory, N., Stuart, J. T. and Walker, W. S., *Philos. Trans. R. Soc. London*, 1955, **248**, 155–199.
14. Gray, W. E., RAE TM Aero 255.
15. Kobayashi, R., Kohama, Y. and Takamadate, Ch., *Acta Mech.*, 1980, **35**, 71–82.
16. Kohama, Y., Proceedings of the 3rd Asian Cong. Fluid Mech., Tokyo, 1986, pp. 162–165.
17. Kobayashi, R., Kohama, Y. and Kurosawa, M., *J. Fluid Mech.*, 1983, **127**, 341–352.
18. Kobayashi, R. and Izumi, H., *J. Fluid Mech.*, 1983, **127**, 353–364.
19. Mueller, T. J., AIAA Paper No. 81-4331.
20. Poll, D. I. A., *Laminar–Turbulent Transition* (eds Eppler, U. and Fasel, H.), Springer-Verlag, 1980, pp. 253–262.
21. Poll, D. I. A., *J. Fluid Mech.*, 1985, **150**, 329–356.
22. Kohama, Y. and Motegi, D., *Exp. Thermal Fluid Sci.*, 1944, **8**, 273–278.
23. Saric, W. S. and Yeats, L. G., AIAA Paper No. 85-0493.
24. Kohama, Y., Ohta, F. and Segawa, K., *Laminar–Turbulent Transition* (eds Arnal, D. and Michel, R.), Springer-Verlag, 1990, pp. 431–440.
25. Kohama, Y., Saric, W. S. and Hoos, J. A., *Trans. JSME No. 91-1704*, 1991, pp. 107–113 (in Japanese).
26. Alfredsson, P. H. and Matsubara, M., *Transitional Boundary Layers in Aeronautics* (eds Henkes, R. A. W. M. and van Ingen, J. L.), Elsiever Science, 1996, pp. 374–386.
27. Kohama, Y. and Ohta, F., *Exp. Thermal Fluid Sci.*, 1994, **8**, 230–238.
28. Kohama, Y. P. *et al.*, Proceedings of the IUTAM Symposium on Laminar–Turbulent Transition, Kluwer, Dordrecht, 2000, to be published.
29. Egami, Y. and Kohama, Y., IUTAM Symposium on Mechanics of Passive and Active Flow Control (eds Meier, G. E. A., Viswanath, P. R.), Kluwer, Dordrecht, 1999, pp. 171–176.
30. Kawakami, M., Kohama, Y. and Okutsu, M., AIAA Paper No. 99-0811.
31. Wlezien, R. W., Parekh, D. E. and Island, T. C., *Appl. Mech. Rev.*, 1990, **43**, 167–174.
32. Saric, W. S., Carrillo, R. B. and Reibert, M. S., IUTAM Symposium on Mechanics of Passive and Active Flow Control (eds Meier, G. E. A. and Viswanath, P. R.), Kluwer, Dordrecht, 1999, pp. 183–188.
33. Kohama, Y. and Egami, Y., AIAA Paper No. 99-0921.